NASA/TM-20210009646 AIAA–2016–4631

Post-Test Inspection of NASA's Evolutionary Xenon Thruster Long-Duration Test Hardware: Discharge and Neutralizer Cathodes

Rohit Shastry and George C. Soulas
Glenn Research Center, Cleveland, Ohio

June 2021

NASA STI Program . . . in Profile

Since its founding, NASA has been dedicated to the advancement of aeronautics and space science. The NASA Scientific and Technical Information (STI) Program plays a key part in helping NASA maintain this important role.

The NASA STI Program operates under the auspices of the Agency Chief Information Officer. It collects, organizes, provides for archiving, and disseminates NASA's STI. The NASA STI Program provides access to the NASA Technical Report Server—Registered (NTRS Reg) and NASA Technical Report Server—Public (NTRS) thus providing one of the largest collections of aeronautical and space science STI in the world. Results are published in both non-NASA channels and by NASA in the NASA STI Report Series, which includes the following report types:

- TECHNICAL PUBLICATION. Reports of completed research or a major significant phase of research that present the results of NASA programs and include extensive data or theoretical analysis. Includes compilations of significant scientific and technical data and information deemed to be of continuing reference value. NASA counter-part of peer-reviewed formal professional papers, but has less stringent limitations on manuscript length and extent of graphic presentations.

- TECHNICAL MEMORANDUM. Scientific and technical findings that are preliminary or of specialized interest, e.g., "quick-release" reports, working papers, and bibliographies that contain minimal annotation. Does not contain extensive analysis.

- CONTRACTOR REPORT. Scientific and technical findings by NASA-sponsored contractors and grantees.

- CONFERENCE PUBLICATION. Collected papers from scientific and technical conferences, symposia, seminars, or other meetings sponsored or co-sponsored by NASA.

- SPECIAL PUBLICATION. Scientific, technical, or historical information from NASA programs, projects, and missions, often concerned with subjects having substantial public interest.

- TECHNICAL TRANSLATION. English-language translations of foreign scientific and technical material pertinent to NASA's mission.

For more information about the NASA STI program, see the following:

- Access the NASA STI program home page at http://www.sti.nasa.gov

- E-mail your question to help@sti.nasa.gov

- Fax your question to the NASA STI Information Desk at 757-864-6500

- Telephone the NASA STI Information Desk at 757-864-9658

- Write to:
  NASA STI Program
  Mail Stop 148
  NASA Langley Research Center
  Hampton, VA 23681-2199

NASA/TM-20210009646 AIAA–2016–4631

Post-Test Inspection of NASA's Evolutionary Xenon Thruster Long-Duration Test Hardware: Discharge and Neutralizer Cathodes

Rohit Shastry and George C. Soulas
Glenn Research Center, Cleveland, Ohio

Prepared for the
52nd Joint Propulsion Conference
cosponsored by the AIAA, ASME, SAE, and ASEE
Salt Lake City, Utah, July 25–27, 2016

National Aeronautics and
Space Administration

Glenn Research Center
Cleveland, Ohio 44135

June 2021

Acknowledgments

The authors would like to thank and acknowledge Kevin McCormick and Jim Sovey for their invaluable aid throughout the post-test inspection process. The authors would also like to thank and acknowledge Pete Bonacuse, Terry McCue, and Joy Buehler of the Analytical Science Group at GRC for their outstanding work involving mounting and polishing samples, SEM imaging, and putting up with our sometimes unreasonable demands on the fidelity of results. Lastly, the authors would like to thank Rob Thomas and Mike Patterson for conducting the additional discharge cathode ignition study mentioned in the paper. This work was funded by the NEXT-C project, which is led by NASA GRC under NASA's Science Mission Directorate.

Level of Review: This material has been technically reviewed by technical management.

Available from

NASA STI Program
Mail Stop 148
NASA Langley Research Center
Hampton, VA 23681-2199

National Technical Information Service
5285 Port Royal Road
Springfield, VA 22161
703-605-6000

This report is available in electronic form at http://www.sti.nasa.gov/ and http://ntrs.nasa.gov/

Post-Test Inspection of NASA's Evolutionary Xenon Thruster Long-Duration Test Hardware: Discharge and Neutralizer Cathodes

Rohit Shastry and George C. Soulas
National Aeronautics and Space Administration
Glenn Research Center
Cleveland, Ohio 44135

Abstract

The NEXT Long-Duration Test is part of a comprehensive thruster service life assessment intended to demonstrate overall throughput capability, validate service life models, quantify wear rates as a function of time and operating condition, and identify any unknown life-limiting mechanisms. The test was voluntarily terminated in February 2014 after demonstrating 51,184 h of high-voltage operation, 918 kg of propellant throughput, and 35.5 MN-s of total impulse. The post-test inspection of the thruster hardware began shortly afterwards with a combination of non-destructive and destructive analysis techniques, and is presently nearing completion. This paper presents relevant results of the post-test inspection for both discharge and neutralizer cathodes. Discharge keeper erosion was found to be significantly reduced from what was observed in the NEXT 2 kh wear test and NSTAR Extended Life Test, providing adequate protection of vital cathode components throughout the test with ample lifetime remaining. The area of the discharge cathode orifice plate that was exposed by the keeper orifice exhibited net erosion, leading to cathode plate material building up in the cathode-keeper gap and causing a thermally-induced electrical short observed during the test. Significant erosion of the neutralizer cathode orifice was also found and is believed to be the root cause of an observed loss in flow margin. Deposition within the neutralizer keeper orifice as well as on the downstream surface was thicker than expected, potentially resulting in a facility-induced impact on the measured flow margin from plume mode. Neutralizer keeper wall erosion on the beam side was found to be significantly lower compared to the NEXT 2 kh wear test, likely due to the reduction in beam extraction diameter of the ion optics that resulted in decreased ion impingement. Results from the post-test inspection have led to some minor thruster design improvements.

Nomenclature

BSE	Backscattered Electron
DCA	Discharge Cathode Assembly
EDS	Energy Dispersive x-ray Spectroscopy
ELT	Extended Life Test
GRC	Glenn Research Center
IPS	Ion Propulsion System
J_B	beam current, A
LDT	Long-Duration Test
LVPI	Low Voltage Propellant Isolator
NCA	Neutralizer Cathode Assembly
NEXT	NASA's Evolutionary Xenon Thruster

NEXT-C	NASA’s Evolutionary Xenon Thruster – Commercial
NEXT LDT	NASA’s Evolutionary Xenon Thruster Long-Duration Test
NSTAR	NASA’s Solar Electric Propulsion Technology Application Readiness
NSTAR LDT	NASA’s Solar Electric Propulsion Technology Application Readiness Life Demonstration Test
PPU	Power Processor Unit
QCM	Quartz Crystal Microbalance
SEM	Scanning Electron Microscopy
V_B	beam power supply voltage, V

1.0 Introduction

NASA has identified the need for a higher-power, higher-specific impulse, higher-thrust, and higher-throughput capable ion propulsion system (IPS) beyond the state-of-the-art NASA Solar Electric Propulsion Technology Application Readiness (NSTAR) IPS employed on the Deep Space 1 and Dawn Missions (Refs. 1 to 4). To fill this need, the NASA’s Evolutionary Xenon Thruster (NEXT) IPS development, led by the NASA Glenn Research Center (GRC), was competitively selected in 2002. The NEXT IPS advanced technology was developed under the sponsorship of NASA’s In-Space Propulsion Technology Program, with Phase 2 close-out of the NEXT IPS development occurring in 2012. The highest fidelity NEXT hardware planned was built by the government/industry NEXT team and includes: an engineering model (referred to as prototype model) thruster, an engineering model power processor unit (PPU), engineering model propellant management assemblies, a prototype gimbal, and control unit simulators (Ref. 5). Each of the units underwent extensive component-level testing, completed environmental testing (with the exception of the PPU), and was tested together in system integration testing (Refs. 6 to 9). Results from IPS component testing and integration testing can be found in References 7 to 17.

The NEXT thruster service life capability is being assessed through a comprehensive service life validation scheme that utilizes a combination of testing and analyses. Since the NEXT thruster is an evolution of the NSTAR thruster design, insights into the operation and erosion processes gained from NSTAR’s development project apply to the NEXT thruster. The NEXT thruster, as a second-generation deep-space gridded ion thruster, made use of over 70,000 h of ground and flight test experience (not including the accumulated hours from the NSTAR IPS on the ongoing Dawn mission) in both the design of the NEXT thruster and evaluation of thruster wear-out failure modes. A NEXT service life assessment was conducted at NASA GRC, employing several models to evaluate all known failure modes with high confidence based upon the substantial amount of ion thruster testing dating back to the early 1960s (Refs. 18 and 19). The NEXT service life assessment also incorporated results from the NEXT 2 kh wear test conducted on a NEXT laboratory model (referred to as engineering model) thruster operating at full power (6.9 kW) (Refs. 18 and 20). The transparency between the engineering model and prototype model thruster wear characteristics was demonstrated by a short-duration prototype model wear test (Ref. 21). The references for the NEXT service life assessment explain the thruster performance and erosion modeling analyses (Refs. 18 and 19).

The NEXT Long-Duration Test (LDT) was initiated in June 2005 as part of the comprehensive thruster service life assessment. The goals of the test were to demonstrate the initial project qualification propellant throughput requirement of 450 kg, validate the thruster service life model’s predictions, quantify thruster performance and erosion as a function of thruster wear and throttle level, and identify any unknown life-limiting mechanisms. In December 2009, after successfully demonstrating the original qualification throughput requirement of 450 kg, the first listed goal was redefined to test to failure of the thruster or until decision to terminate the test voluntarily.

A decision to voluntarily terminate the test was made in April 2013 due to budget constraints. After a comprehensive end-of-test performance characterization was completed (Ref. 22), the thruster was vented to atmospheric conditions in April 2014. At the end of the test, the thruster had accumulated 51,184 h of high-voltage operation, processed 918 kg of xenon propellant, and delivered 35.5 MN-s of total impulse, setting numerous records for the most demonstrated lifetime of an electric propulsion device. Post-test inspection of the hardware was initiated soon after removal of the thruster from the vacuum facility. The results of this inspection for both the discharge and neutralizer cathodes are the subject of this paper. Results for other thruster components, including the ion optics and discharge chamber, and covered in companion publications (Refs. 23 and 24).

In April 2015, Aerojet Rocketdyne (with subcontractor ZIN Technologies) was competitively selected for the NASA's Evolutionary Xenon Thruster – Commercial (NEXT-C) contract. The objectives of this contract are two-fold: 1) To deliver two flight thrusters and two flight PPUs for use in future NASA missions, and 2) take steps to transition NEXT into a commercially available, off-the-shelf IPS for use by NASA as well as other interested parties. While the LDT was initiated as part of the Phase 2 effort under NASA's In-Space Propulsion Technology Program, the post-test inspection of the LDT thruster hardware has now fallen under the NEXT-C contract to be performed as an in-house task by GRC. The results of the LDT will then be relayed to Aerojet Rocketdyne along with any recommended design improvements to be made to the thruster flight design.

The paper is organized as follows: Section 2.0 covers the background for the NEXT LDT, including details of the test article as well as the throttling profile used over the course of the test. Section 3.0 describes the post-test inspection objectives, as well as the overall approach that was taken. Section 4.0 includes major results of the post-test inspection for the discharge and neutralizer cathodes, including resolution of several issues encountered during the test. Section 5.0 then summarizes key findings and briefly describes remaining future work.

2.0 NEXT Long-Duration Test Background

The NEXT LDT was conducted within Vacuum Facility 16 at NASA GRC. The test article is a modified version of an engineering model (designated EM3), shown firing in Figure 1. To obtain a flight-representative configuration, prototype-model ion optics were incorporated, provided by industry partner Aerojet Corporation (now Aerojet Rocketdyne). A graphite discharge cathode keeper electrode was also incorporated into EM3 (Ref. 25). The NEXT thruster is nominally a 0.5 to 6.9 kW input power xenon thruster utilizing 2-grid dished-out ion optics, capable of producing thrust levels of 25 to 235 mN and specific impulses of 1400 to 4160 s. The technical approach for NEXT continues the derating philosophy used for the NSTAR ion thruster. A beam extraction area of 1.6X that of NSTAR allows for higher thruster input power while maintaining low discharge voltages and ion current densities, thus maintaining thruster longevity. Additional descriptions of the hardware, including the NEXT EM3 design and vacuum facility, can be found in References 2, 26, 27 to 31.

Various diagnostics were utilized to characterize the performance and wear of the thruster during the LDT. These include: three staggered planar probes on a single-axis motion table to monitor ion current density distributions and beam divergence, a quartz crystal microbalance (QCM) to monitor backsputtered efflux from the facility, and an E × B probe to monitor the charge-state signature of the thruster plume. A data acquisition and control system was also used to monitor the thruster telemetry at 15 Hz and permit autonomous operation. A set of six in situ, charge-coupled device cameras were placed on the single-axis motion table to monitor wear rates of critical components on the thruster. These cameras imaged the downstream neutralizer keeper and cathode orifice plates, the discharge keeper and cathode orifice plates, accelerator grid apertures at various radials locations from centerline, and the cold grid gap of the ion optics. Additional details of the testing and facility diagnostics can be found in References 29 and 32.

The NEXT IPS was designed for solar electric propulsion applications that experience variable input power as the available solar flux changes with distance from the sun throughout the mission. For the LDT, the EM3 thruster was operated in a mission-representative profile comprised of discrete segments at various power levels shown in Table I and described in detail in Reference 33. The thruster was operated at each of these segments for sufficient duration to characterize the performance and wear rates, and to validate the thruster service life models. The throttle profile was completed in May 2010 and the thruster was then operated at full power until the end of the test in February 2014. For the majority of the test, detailed performance characterizations were carried out at 11 of the 40 operating conditions in the NEXT throttle table. These characterizations included overall thruster performance as well as component performance of the discharge chamber, neutralizer cathode, and ion optics. A comprehensive performance characterization was also performed at the end of the test that included all 40 operating conditions in the NEXT throttle table. Details of performance measurements as well as in situ images taken during the test can be found in References 22, 28, 29, 32 to 40.

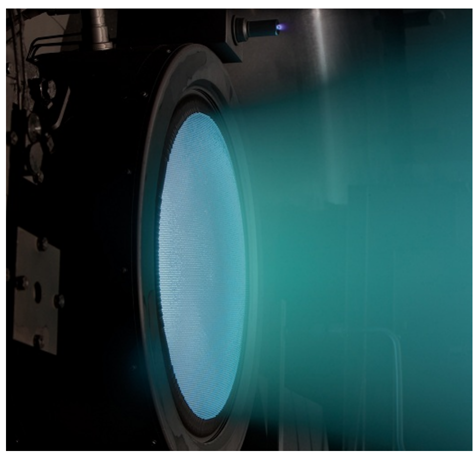

Figure 1.—Photograph of NEXT EM3 firing within Vacuum Facility 16 at GRC.

TABLE I.—NEXT LONG-DURATION TEST MISSION-REPRESENTATIVE THROTTLING PROFILE

Throttle segment	Throttle level	Input power, kW	Operating condition (J_B, V_B)	Segment duration, kh	End of segment date
1	TL40	6.9	3.52 A, 1800 V	13.0	11/17/2007
2	TL37	4.7	3.52 A, 1179 V	6.5	12/23/2008
3	TL05	1.1	1.20 A, 679 V	3.4	06/24/2009
4	TL01	0.5	1.00 A, 275 V	3.2	12/15/2009
5	TL12	2.4	1.20 A, 1800 V	3.1	05/05/2010
6	TL40	6.9	3.52 A, 1800 V	21.9	02/28/2014

3.0 Post-Test Inspection Objectives and Approach

The post-test inspection for the NEXT LDT largely followed the same approach and processes as what was employed for the inspection of the NSTAR Extended Life Test (ELT) thruster hardware (Ref. 41). The primary objectives of the post-test inspection are to: measure critical thruster wear rates that can induce thruster failure, to verify both in situ measurements and the service life model predictions; resolve any thruster-related issues encountered during the NEXT LDT; verify that thruster design changes made as a result of prior wear test findings had the desired impacts; and identify any unanticipated life-limiting phenomena. The thruster components were first inspected non-destructively in order to preserve the hardware for potential future testing. It was originally thought that resolution of issues encountered during the test or further characterization of the state of the hardware may require additional operation of individual components or the thruster as a whole. However, after reviewing results from the non-destructive inspection, it was determined that resolution of many open issues and questions required destructive inspection of various thruster components.

Particular attention was paid to failure modes that were identified during the initial lifetime assessment and service life modeling for the NEXT thruster (Ref. 18). For the cathodes, these failure modes included: insert barium depletion resulting in excessive cathode temperatures or inability to ignite; excessive wear of the keeper orifice plate (discharge cathode) or keeper tube (neutralizer cathode) resulting in exposure of the cathode orifice plate and heater; excessive wear of the cathode orifice plate; heater mechanical failure from cyclic operation; and neutralizer cathode orifice clogging preventing proper cathode operation.

Each hollow cathode contains an electron emitter impregnated with barium oxide, calcium oxide, and aluminum oxide. Migration of barium and barium oxide to the surface reduces the surface work function, allowing the necessary electron emission to occur at reduced temperatures. Barium at the surface is lost through evaporation and eventually becomes depleted at the downstream end of the cathode, forcing the reaction front to move further upstream. If sufficient barium loss occurs, the surface work function increases and required cathode operating temperatures rise. If the cathode heater can no longer produce the necessary temperatures, the cathode will no longer be able to ignite. Characterization of the barium depletion within each cathode insert for the LDT is presently ongoing, with results to be presented at a later date. However, given the typical ignition times that were observed throughout the test, excessive barium depletion in either cathode is not expected.

Erosion of the downstream face of the keeper orifice plate on the discharge cathode occurs from sputter erosion by ions formed downstream of the cathode. This erosion was so severe during the NSTAR ELT that the keeper orifice plate had completely eroded away by the end of the test. Because the primary purpose of the discharge keeper in NSTAR is to protect the cathode orifice plate and heater coil from ion bombardment, the excessive erosion of the keeper also led to sputter erosion of the cathode orifice plate, heater coil, and radiation shield (Ref. 41). Erosion of the keeper orifice plate was also found to be higher than expected during the NEXT 2 kh wear test (Ref. 20). To increase cathode lifetime, the keeper material was changed from a refractory metal to a carbon-based material with a significantly lower sputter yield. This change was made to the EM3 hardware that was tested during the NEXT LDT.

While the downstream face of the keeper orifice plate on the neutralizer cathode has not been found to erode in past NSTAR and NEXT life tests, the side of the keeper tube facing the ion beam is vulnerable to sputter erosion. Excessive erosion of this surface was found during the NEXT 2 kh wear test (Ref. 20). While wear through the keeper tube thickness does not cause cathode failure, in order to increase cathode lifetime the keeper tube thickness was increased by 50 percent; however, this design change was not implemented on the EM3 hardware. Due to excessive erosion of outer radius apertures on the accelerator grid observed during the NEXT 2 kh wear test, the ion extraction diameter was reduced from 40 to 36 cm. This change, employed on the EM3 prototype-model ion optics, should reduce the wear rate on the beam side of the neutralizer keeper tube.

If excessive erosion of the keeper electrode occurs, it may expose areas of the cathode orifice plate to ion bombardment. Furthermore, the downstream portion of the cathode orifice plate exposed by the keeper orifice is immediately vulnerable to sputter erosion by ions. Erosion of the cathode orifice plate could either result in structural failure, or inability to operate due to significant changes to the geometry of the orifice (e.g., enlargement).

Heater coils are used to heat the cathode and emitter to sufficient temperatures required for ignition. Once ignited, the discharge provides sufficient heating to keep the cathode ignited and the heater may be turned off. After a certain number of these cycles, heaters can mechanically fail, preventing them from conducting the required current to heat the cathode. For the NEXT (and NEXT-C) projects, heaters are cyclically tested separately in order to quantify their lifetime. Ignition times are typically no longer than 6 min, and heaters made for the NEXT project in the past have demonstrated in excess of 6,000 cycles (Ref. 13). Because the NEXT LDT had approximately 350 ignitions over the course of the test, heater damage due to excessive cycling is not expected.

Neutralizer cathode orifice clogging was observed during low power (i.e., low beam current) operation in the NSTAR ELT (Ref. 41). Unfortunately, the material causing the clogging was removed during subsequent operation at full power, preventing investigation of the cause during post-test inspection. Excessive clogging of the orifice may prevent proper cathode operation. However, such clogging was not observed during the NEXT 2 kh wear test or the NEXT LDT, and given that the orifice diameter on the NEXT neutralizer is nearly twice that of the orifice diameter on the NSTAR neutralizer, orifice clogging on NEXT is unlikely (Refs. 18, 20, and 22).

Apart from verification of the increased component lifetime gained from the design changes described above, the post-test inspection of the hardware was needed to resolve a number of issues encountered during the test. In particular, causes needed to be determined (or verified) for: an observed cathode-to-keeper electrical short and heater open circuit in the discharge cathode; a low impedance between the neutralizer and facility ground; and a loss of neutralizer performance (flow margin from plume mode operation) over the course of the test. These issues and their resolution, as well as other pertinent results, are described in the next section.

4.0 Results and Discussion

4.1 Discharge Cathode

4.1.1 General Inspection

The discharge cathode assembly (DCA) was visually inspected after removal of the ion optics from the thruster. Figure 2 shows a photograph of the discharge cathode prior to removal from the discharge chamber. The discharge keeper, whose primary purpose in NEXT is to protect internal cathode components from the discharge plasma, appeared intact with little erosion, even after 51.7 kh of cathode operation. The exposed portion of the cathode orifice plate had a highly textured appearance, exhibiting a bowl-like shape that indicates significant erosion. Substantial deposition was also found within the gap between keeper and cathode plate surfaces, at a location coincident with the keeper orifice circumference. All of these features are discussed in more detail in the sections below.

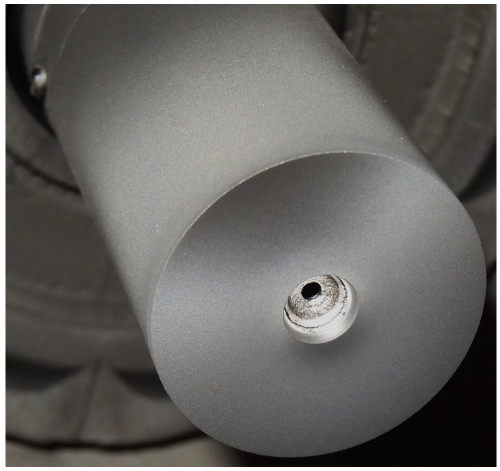

Figure 2.—Photograph of the discharge cathode within EM3 shortly after the ion optics were removed.

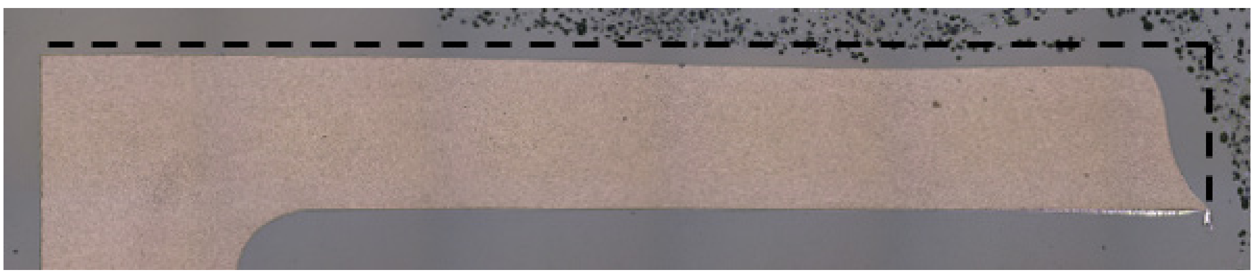

Figure 3.—Cross section of the discharge keeper orifice plate from the NEXT LDT. The top corresponds to the downstream surface, with the dashed line indicating the nominal pretest profile.

Geometric and magnetic field measurements in the vicinity of the cathode indicated that the DCA did not shift during the test and was still properly positioned within the magnetic field of the discharge chamber. All electrical connections were checked and found to be secure, and no issues were found with any of the electrical insulators. Lastly, the discharge cathode flow line (including all fittings) was checked for leaks and none were found.

4.1.2 Discharge Cathode Keeper

To characterize the final geometry of the discharge keeper from the NEXT LDT, it was axially cross-sectioned through the center and inspected with an optical microscope. Non-contact profilometry of the downstream surface was first performed across four diameters. The orifice plate was then mounted in epoxy to ensure that any deposition was minimally disturbed during the sectioning process. Figure 3 shows a photograph of one side of the keeper orifice plate cross section, with a dashed lined indicating the nominal pretest profile for reference. It is evident from the figure that erosion had occurred across the entire downstream face as well as within the keeper orifice. The eroded downstream profile exhibits a shape very similar to that found during the NSTAR Life Demonstration Test (LDT) and the NEXT 2 kh wear test (Refs. 20 and 42). However, the maximum eroded depth is only 15.8 percent of the pretest thickness, occurring at a location of 39 percent of the total radius. There was no observable erosion or deposition on the cathode keeper tube wall. These results are remarkably similar to those found in the NEXT 2 kh wear test, with a maximum eroded depth of 17 percent of the thickness at a location of 40 percent of the total radius. This indicates that the keeper material change has successfully provided a

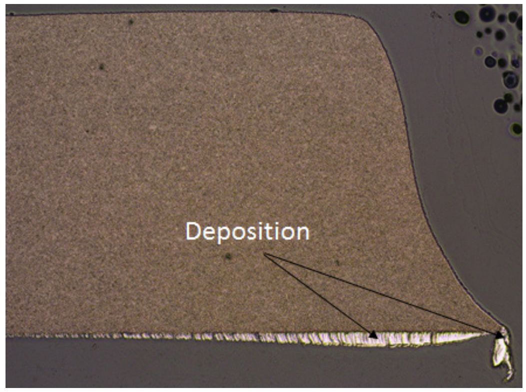

Figure 4.—Close-up view of the discharge keeper orifice cross section. The entire orifice shows net erosion, and deposits were found on the upstream side of the orifice plate.

substantial increase in the lifetime over what was observed in the NSTAR LDT, NSTAR ELT, and NEXT 2 kh wear tests.

Figure 4 shows a close-up photograph of the keeper orifice. It is evident from this figure and Figure 3 that the orifice has enlarged throughout nearly the entire plate thickness. However, a deposition layer approximately 2 μm thick was found on the upstream portion of the orifice barrel, covering 20 percent of the original keeper thickness. This layer indicates that the upstream part of the orifice was not continually eroding throughout the test. The minimum diameter within the orifice was measured using a non-contact method to be within 0.4 percent of the pretest diameter. For comparison, the in situ measurement of the keeper orifice diameter taken at the end of the test indicated a decrease of 3 percent, which is in agreement with the post-test value within the measurement uncertainty.

Deposition on the upstream surface of the keeper orifice plate is also evident from Figure 4. This deposition reached a maximum thickness of 4.2 percent of the pretest keeper orifice plate thickness. This excludes the deposition "hanging" from the upstream corner of the keeper orifice. It is unknown if that deposition, which is 12.9 percent of the pretest keeper plate thickness, was disturbed during the post-test inspection. However, it is likely that what is shown in Figure 4 resembles the true geometry because the orifice plate was mounted in epoxy prior to sectioning, and the deposition was found to be tightly adhered to the substrate. Energy dispersive x-ray spectroscopy (EDS) indicated that this deposition was material from the cathode orifice plate. This deposition is believed to have been responsible for the intermittent cathode-to-keeper electrical short observed during the test. This is discussed in further detail in Section 4.1.4.

4.1.3 Discharge Cathode Orifice Plate and Tube

The discharge cathode orifice plate and tube were visually inspected after the keeper was removed from the DCA. Figure 5 shows a photograph of a face-on view of the discharge cathode orifice plate with the keeper removed. The area that was exposed to the discharge plasma by the keeper orifice has a textured appearance and is a region of net erosion. Near the perimeter of this area, roughly coincident with the diameter of the keeper orifice, there is a ridge of deposition flaring outward from the orifice plate surface. This deposition was found to be highly fragile, and was only loosely bound to the cathode orifice plate. Outside of the region of net erosion, there is no visual wear due to operation. In fact, machining marks on the surface are still visible. This is a significant improvement over the erosion observed in the NSTAR ELT, where the outer edge of the plate was only 28 percent of the pretest plate thickness and was only attached to the cathode tube by a 20 to 50 μm wide fused area. The cathode orifice plate was completely exposed to the discharge plasma during the NSTAR ELT due to excessive keeper plate erosion (Ref. 41).

Non-contact profilometry was performed on the downstream surface across four diameters. Afterwards, the cathode orifice plate and tube were mounted in epoxy (to prevent disturbing deposition material) and sectioned through the tube centerline. Material from the deposition ridge on one side was preserved prior to the mounting and sectioning process. Figure 6 shows the cross section of the discharge cathode orifice plate, with the nominal pretest geometry provided for reference. Much of the original chamfer as well as portions of the downstream surface exposed by the keeper had been eroded. However, the cylindrical portion of the orifice shows significant net deposition. Based on EDS analysis, this material either came from the cathode insert or the orifice plate itself. However, no insert impregnate material (i.e., barium, calcium or aluminum) was found in the deposition, so it is more likely that the source was eroded products from cathode plate surfaces further downstream.

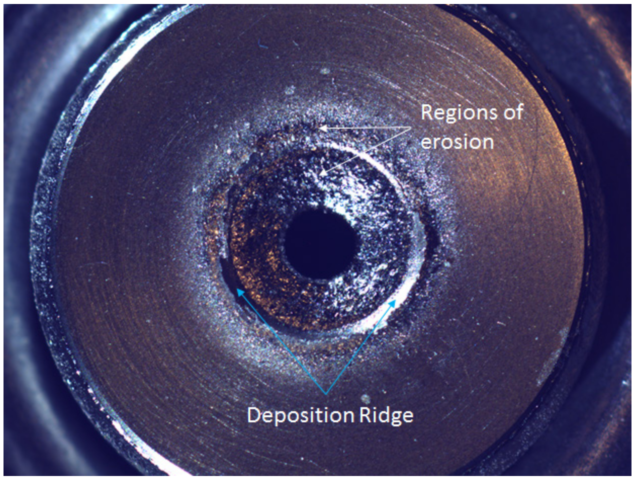

Figure 5.—Face-on view of the discharge cathode orifice plate after the keeper was removed from the assembly. The area exposed by the keeper orifice exhibits net erosion, with a distinct deposition ridge near the perimeter.

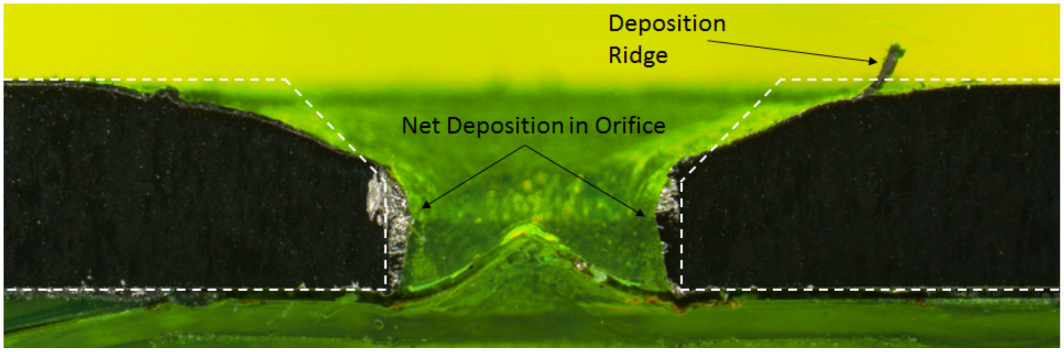

Figure 6.—Discharge orifice plate cross section through centerline. The dashed lines correspond to the nominal pretest plate geometry. Net deposition was observed within the upstream orifice barrel.

A non-contact measurement technique performed prior to sectioning indicated that the minimum cathode orifice diameter had decreased by 13 percent compared to the pretest diameter. In situ measurements taken at the end of the test prior to venting the facility indicated that the orifice diameter reduced by 5 ± 3.5 percent. The discrepancy, even after accounting for measurement uncertainty, is presently unknown. It is possible the in situ camera for the DCA either did not have the resolution to fully define the cathode orifice edge as it eroded or had insufficient lighting to see through the entire thickness of the plate. A reduction in the minimum cathode orifice diameter was not entirely unexpected, as similar reductions were found during the NEXT 2 kh wear test and NSTAR LDT, measuring 3 and 5 percent less than pretest diameters, respectively. However, for these tests the source of deposits appear to have come from the keeper and insert (Refs. 20, 42, and 43). The cathode orifice chamfer diameter was also measured with in situ cameras throughout the test. However, as seen in Figure 6, the outer edge of the chamfer is no longer well-defined. Comparison of in situ images to those taken during the post-test inspection indicate that the boundary being tracked as the chamfer diameter later in the test was likely the inner edge of the deposition ridge (Ref. 22).

Based on Figure 5 and Figure 6, the deposition ridge is positioned within the eroded zone, and not on the outside perimeter. This indicates that the deposition ridge had formed on the cathode surface after the substrate had eroded, at least to a degree. There also appears to be an inflection point in the eroded chamfer of the cathode orifice plate in the vicinity of the deposition ridge, possibly caused by the deposition shadowing the orifice plate at larger radii, preventing further erosion. This provides insight into the way this deposition developed, which is believed to be responsible for the observed cathode-to-keeper electrical short during the test. This topic is discussed in more detail in Section 4.1.4.

Trace amounts of deposition were found on the downstream surface of the cathode orifice plate as well as within the cathode tube. Analysis using EDS indicates that these deposits were composed of either cathode orifice plate material and/or material from the cathode insert. Insert material within the cathode tube is not surprising given that the insert tube is in close proximity with most of the surface. Unfortunately, it appears that much of this material was very loosely adhered to the surface, and flowed freely while the cathode tube was being mounted in epoxy (the material used for mounting is a liquid that then sets and cures). An artifact of this mounting technique can be seen in Figure 6 within the cathode orifice, where a liquid “front” can be seen emanating from the upstream surface of the orifice plate into the middle of the orifice. While it is unfortunate that not all of the deposits could be preserved by mounting the piece in epoxy, the structure of the deposits within the orifice and of the deposition ridge were able to be captured with this technique.

4.1.4 Discharge Cathode-Keeper Electrical Short

An electrical short between the discharge cathode and keeper was observed during the NEXT LDT. This short began as a thermally-induced short, beginning to manifest during ignitions around 13 kh. Around 48 kh, the short developed from being thermally-induced to a more consistent short present even at room temperature (Ref. 40). This shorting was not entirely unexpected given results from similar discharge cathodes in the NEXT 2 kh and High Power Electric Propulsion 2 kh wear tests at GRC, which showed deposits on the upstream surface of the keeper orifice plate (Refs. 43 and 44). Cathode-to-keeper shorting was also observed during the NSTAR ELT between approximately 6 to 9 kh. It was presumed that the short had cleared afterwards due to sufficient keeper orifice erosion (Ref. 41).

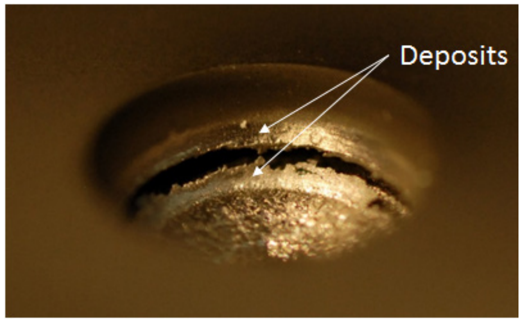

Figure 7.—Photograph of the discharge cathode-keeper gap, revealing significant deposits originating from the cathode orifice plate.

Post-test inspection of the discharge cathode revealed significant deposits in the gap between the cathode and keeper orifice plates (see Figure 7). Once the keeper electrode was removed from the cathode assembly, high impedance (~ 52 GΩ at maximum operating voltage) was measured between keeper and cathode common. This indicates that the bridging material, not other components such as the wiring or electrical insulators further upstream, was responsible for the electrical short observed during the test. Analysis of these deposits with EDS revealed they had come from the cathode orifice plate. It is speculated that erosion of the exposed surface of the cathode orifice plate deposited material on the upstream surface of the keeper orifice plate. Over the course of the test, this material thickness grew until it made contact with the cathode orifice plate during ignitions. The deposits then subsequently "tore" and left behind material that had bonded to the downstream surface of the cathode orifice plate. This explanation is supported by the observation that the deposition on the keeper was tightly adhered while the deposition on the cathode orifice plate was loosely bound. Furthermore, the deposition was bonded in a region of the cathode orifice plate exhibiting erosion, indicating that it likely did not begin accumulating on that surface.

Given that the material originated from the cathode orifice plate, this short is expected to develop in flight. During the test, the presence of the cathode-keeper short appeared to increase cathode ignition times (Ref. 22). This is expected to be the only significant effect of the short on thruster performance or lifetime. In order to better quantify the impact the short had on ignitions, conditions for each of the 350 ignitions from the test were characterized in order to isolate the effect of the cathode-keeper short. It was found that additional factors, such as facility regenerations and the presence of a heater open circuit, had contributed to increased ignition times and tended to obfuscate the true impact of the short.

Figure 8 provides histograms of ignition times for "nominal" ignitions where no issues were present (also excludes ignitions performed directly after a facility regeneration), as well as ignitions where a cathode-keeper short was the only issue present (excludes post-regeneration ignitions, ignitions where the heater went open-circuit, and ignitions considered "atypical" due to factors such as operator error). For nominal ignitions, 185 ignitions took place with an average ignition time of 3 min 44 s and a maximum of 8 min and 53 s. For ignitions where the keeper was shorted to cathode, 50 ignitions took place with an average ignition time of 6 min 5 s and a maximum of 28 min. These data indicate that the short does increase ignition time, but by an average of ~ 2.5 min. An ongoing ignition study is presently being performed on engineering model NEXT hardware to provide additional data that characterizes the impact of a cathode-keeper short on ignition time. The preliminary results of this study also indicate that the presence of an electrical short increases ignition times by ~ 2 min on average (Ref. 45).

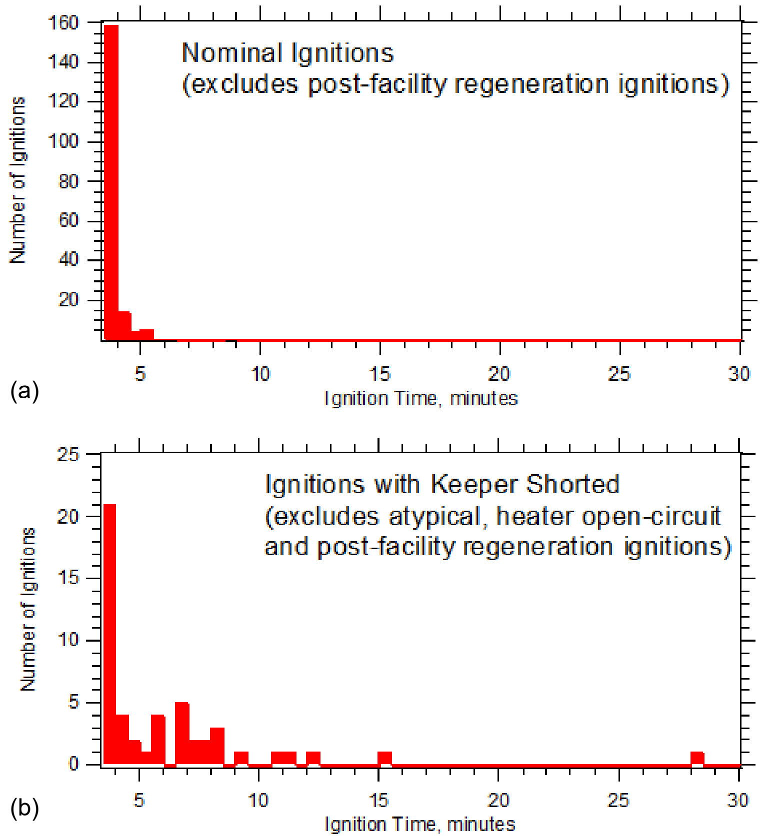

Figure 8.—Histograms of discharge ignition times from the NEXT LDT. (a) Ignition time distribution of nominal ignitions with no issues present. Average ignition time was 3 min 44 s. (b) Ignition time distribution with the cathode-keeper short being the only issue. Average ignition time was 6 min 5 s.

It is worth noting that during both the NEXT LDT and this additional study, long electrical line lengths between the thruster and power supplies had attenuated the ignitor voltage pulse by nearly a factor of two. This could have a significant effect on ignition times, especially when the keeper is shorted to the cathode. Additional studies are currently planned to deliver the nominal ignition pulse voltage to the thruster and determine if the impact of the short on ignition times is reduced.

As mentioned previously, a short between the discharge cathode and keeper was observed during the NSTAR ELT. This short had disappeared after 9 kh, presumably due to enlargement of the keeper orifice. However, due to the excessive erosion of the discharge keeper observed during the NSTAR ELT, the keeper material was changed to one with a much lower sputter yield for thrusters on the Dawn mission. While this change would significantly increase keeper lifetime on the NSTAR thruster, it is more likely that cathode-keeper shorts would develop and persist in flight. Unfortunately, such a measurement is not available on the Dawn spacecraft so it is unknown whether a cathode-keeper short has occurred. However, to-date there have been 653 thruster starts across three thrusters, will all ignitions occurring within 1 s of commanding the ignitor voltage pulse (Ref. 46). This indicates that even if a cathode-keeper short is present, it may not have an impact on ignition times in flight.

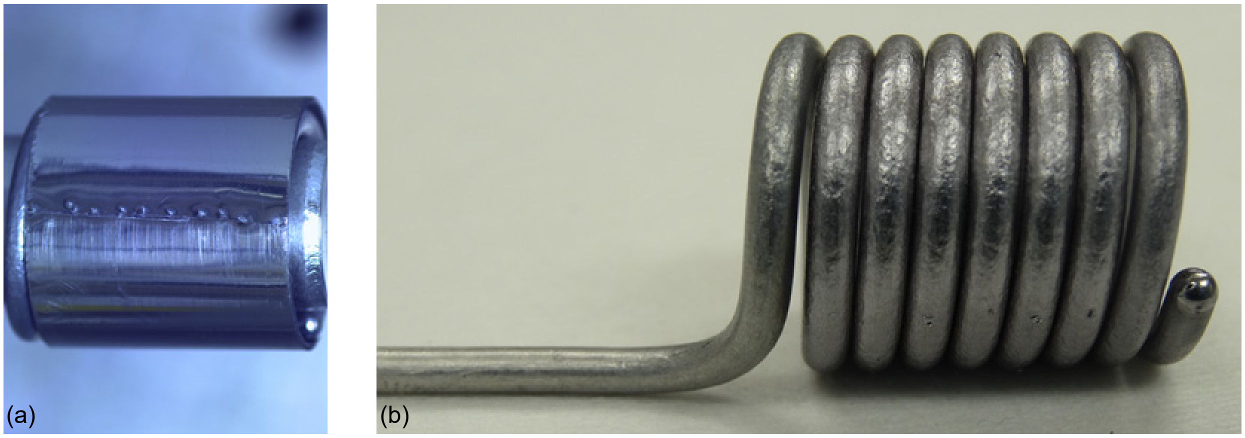

Figure 9.—Photographs of (a) the DCA heater radiation shield and (b) the heater coil after removal from the cathode tube. No visible wear or defects were found to be caused by cathode operation.

4.1.5 Discharge Cathode Radiation Shield and Heater

The exposed cathode heater and radiation shield were visually inspected after the keeper was removed from the DCA. Figure 9 shows photographs of these two components during post-test inspection. The radiation shield was found to be in remarkably good condition, with no visual indications of any wear. The heater coil was also in excellent condition, with both heater terminations intact. Post-test measurements of the heater coil resistance (prior to removal from the cathode assembly) using a milliohmeter yielded an average value of 0.452 Ω, which is only 1.5 percent lower than the pretest value of 0.459 Ω and within the measurement variation. This lack of observable wear is not surprising. Given the minimal amount of erosion found on the discharge keeper, it had adequately protected the cathode orifice plate, heater coil and radiation shield from the discharge plasma during thruster operation for over 51 kh. This is a marked improvement over what was observed in the NSTAR ELT, which had significant damage to these components due to excessive keeper erosion and subsequent exposure to the discharge plasma (Ref. 41).

During the NEXT LDT, an intermittent, thermally-induced discharge heater open circuit was observed during cathode ignitions from ~ 13 to 29 kh. This open circuit typically caused increased cathode ignition times. It had been speculated that this open circuit was caused by poor contact between the heater sheath and the cathode tube. For the engineering model cathode, a “friction fit” contact between the heater coil and the downstream end of the cathode tube was used as the only return path for heater current (Ref. 32). It was speculated that initial thermal expansion of the heater coil during the ignition procedure had caused the heater to momentarily separate from the cathode tube, resulting in the open circuit. As heat is transferred to the cathode tube, it expands as well until contact with the heater is reestablished.

Visual inspection of the interface between the heater coil and the cathode tube could not verify the presence of any gap (although this was only done at room temperature). However, comprehensive measurements of the resistance across various components in the heater circuit on the cathode indicated that all connections were secure and resistances were repeatable except for the one between the heater sheath and cathode tube, which was highly variable and sometimes exceeded 20 Ω at room temperature. This large variation indicates poor contact between the heater sheath and cathode tube, supporting the speculated cause for the open circuit behavior observed during the test. Furthermore, during destructive disassembly the heater coil was easily removed from the cathode tube with little to no force, also indicating a loose or poor contact between the two components.

While the lack of a positive return path is an issue for the engineering model discharge cathodes, it is not expected to occur for the NEXT flight cathodes. The present flight design incorporates a more reliable, secure connection between the cathode tube and heater sheath, and Aerojet Rocketdyne is working to ensure such a connection is adequate in preventing heater open circuits during ignitions and cathode conditioning sequences.

4.2 Neutralizer Cathode

4.2.1 General Inspection

The neutralizer cathode assembly (NCA) was inspected prior to removal from the thruster. Most of the exposed keeper surface was coated with deposition, including the downstream face of the orifice plate (see Figure 10). Spalling of deposition films was also evident on the downstream face of the neutralizer enclosure. These films were comprised of backsputtered material from the facility walls, and are therefore not expected in flight. Deposition on the keeper was expected, as the majority of the neutralizer keeper has not been a site of significant erosion (Refs. 18, 20, and 41). The exception is the side of the keeper facing the ion beam, which can be susceptible to direct ion beam impingement. Figure 10(b) shows the region of the beam-side of the keeper tube that exhibited net erosion. Furthermore, the downstream edge of the tube from 3 o'clock to 9 'clock (bottom half facing the thruster beam) exhibited a roughened appearance. This was determined to be the deposition on the downstream face fragmenting as it transitions to the region of net erosion on the beam-side of the tube. The exposed part of the neutralizer cathode orifice plate also exhibited a heavily textured appearance, with noticeable erosion occurring in the chamfer region of the orifice. All of these features are discussed in more detail in the corresponding sections below.

All electrical connections and wiring were inspected and no issues were found. This was important to verify due to the observed low impedance between neutralizer common and facility ground during the test. The mass flow line was also checked and no significant leaks were found. This was also important as a leak in the flow line could explain the loss in performance (decrease in flow margin from plume mode) that was observed during the test, so this was eliminated as a possibility. These issues and their resolution are discussed in further detail in the sections below.

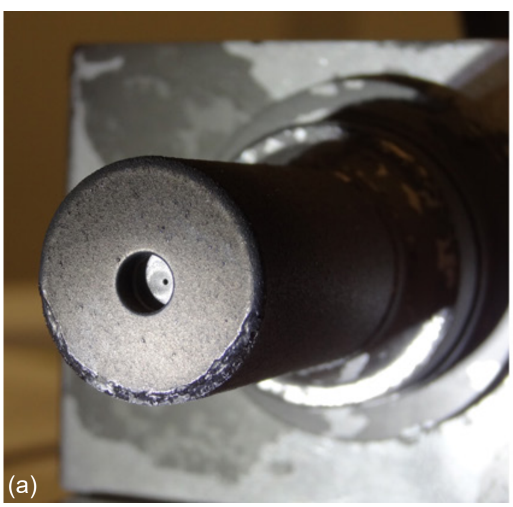

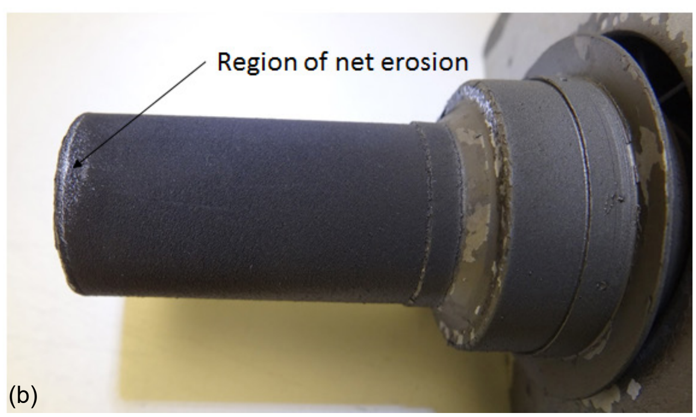

Figure 10.—Photographs of the NCA during the post-test inspection prior to disassembly. (a) Front view of the neutralizer, showing deposition on most of the keeper surface. The thruster would be at the bottom of the image. (b) Side view of the neutralizer keeper tube facing the ion beam, showing a region of net erosion near the orifice plate.

4.2.2 Neutralizer Cathode Keeper

The neutralizer keeper was removed from the assembly and sectioned axially through the center to determine its final geometry. The section was mounted in epoxy prior to polishing in order to preserve the deposition present on most surfaces. Prior to sectioning, the minimum diameter of the keeper orifice was measured using a non-contact technique, indicating that the keeper diameter had decreased by 6 percent. This is inconsistent with in situ measurements taken at the end of the test prior to venting the facility, which had indicated that the diameter had increased by 1 percent (essentially no change given the measurement uncertainty). The reason for this discrepancy is presently unknown.

Figure 11 shows a cross section of the neutralizer keeper near the orifice. It is evident from the photograph that deposition is present on all surfaces. The deposition layer on the downstream face of the orifice plate, determined by EDS analysis to be primarily carbon from the facility, was measured to be approximately 27 percent of the pretest keeper thickness. This is significantly higher than the estimated deposition thickness using QCM data taken during the test (Ref. 22). The reason for this discrepancy is presently unknown. While the calculated thickness from the QCM data assumes that carbon is deposited at the maximum theoretical density, the deposition observed on the downstream face of the keeper does not appear to be porous. Deposition films sampled away from the thruster, such as on the facility endcap behind the thruster, have overall thicknesses consistent with the calculated thickness from QCM data. Therefore, it is possible that plasma conditions in the vicinity of the cathode enable a higher deposition rate than what is measured by the QCM placed at the side of the thruster. However, the deposition thickness observed on the downstream face of the neutralizer in the NSTAR ELT was consistent with the calculated thickness from a QCM (Ref. 41).

Deposition within the orifice, seen in Figure 11, was verified to be responsible for the measured decrease in orifice diameter prior to sectioning. This deposition, determined using EDS to be a mixture of backsputtered carbon from the facility as well as material from the cathode orifice plate, was also found on the upstream side of the keeper orifice plate. The maximum thickness on the upstream side was found to be 6 percent of the pretest keeper thickness, and tapers off rapidly with increasing radial distance from the orifice. Figure 12 shows a backscattered electron (BSE) photomicrograph of the deposition within the keeper orifice. The overall deposition exhibits a jagged appearance that is qualitatively similar to what was observed in the NSTAR ELT (Ref. 41). As a BSE image, lighter areas in Figure 12 correspond to

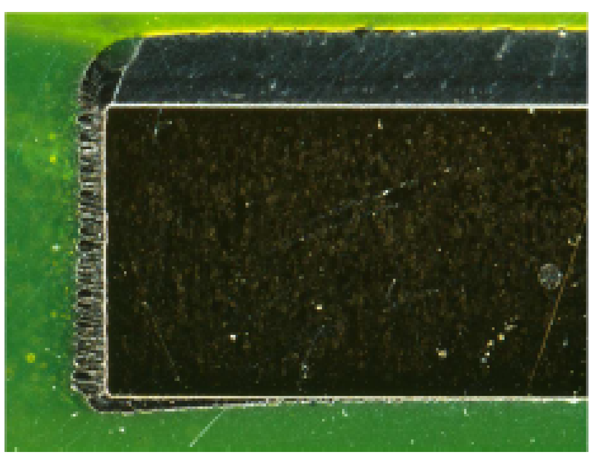

Figure 11.—Cross section of the neutralizer keeper orifice plate near centerline. The orifice is to the left, while the downstream face is at the top. Deposition was observed on all surfaces.

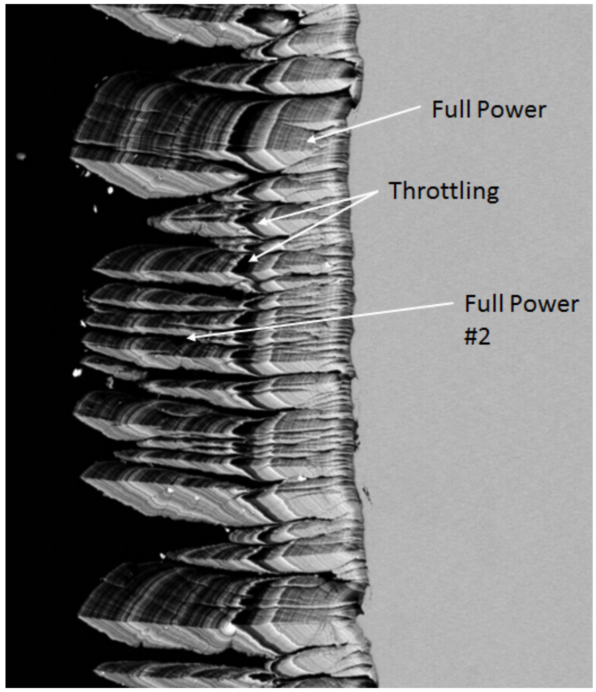

Figure 12.—Backscattered electron image of the deposition found within the neutralizer keeper orifice.

heavier elements (i.e., material from the cathode orifice plate) while darker areas correspond to lighter elements (i.e., backsputtered carbon from the facility). The deposition within the orifice exhibits a layering that is similar to what was observed on the screen and accelerator grids from the NEXT LDT (Ref. 23). This layered appearance was correlated to the throttling of the thruster over the course of the test. The relative amounts of heavy and light elements in each layer are dependent upon the thruster erosion rates and facility backsputter rates. Given the composition of the deposition in each layer, it is likely that the highest level of cathode orifice plate erosion rates occurred at a beam current of 3.52 A during the first 19.5 kh of operation. This is consistent with performance and in situ camera data, which show the largest changes in neutralizer performance and orifice chamfer dimensions occurring during this time (Ref. 22). The overall changes to the dimensions of the keeper orifice plate due to deposition were higher than anticipated. The increase in effective keeper thickness and decrease in effective keeper diameter and keeper-to-cathode gap could improve neutralizer performance and partially mask the loss in performance observed during the test. Thus, this deposition may be partially responsible for the relatively constant neutralizer performance observed during the last 10 to 15 kh of the test. Because much of this deposition is a facility effect and will not be present in flight, its impact on the measured performance loss during the LDT will need to be assessed.

One of the potential failure modes listed in Section 3.0 was erosion of the neutralizer keeper tube, exposing the cathode orifice plate and heater. General inspection of the keeper indicated a net erosion zone on the beam side of the keeper tube. Figure 13 shows a cross section of this region, illustrating the thinning of the keeper tube wall due to ion impingement. A photograph of the opposite side is provided for comparison, which shows no thinning and slight deposition. Also evident in the figure is the breaking of the deposition layer on the downstream face of the keeper orifice plate as it transitions into the net erosion region on the beam side of the tube. To quantify the level of erosion, the radial distance from the outer surface to a reference plane (taken as the inner surface of the tube wall) was measured as a function of distance from the downstream face of the keeper orifice plate substrate (see Figure 14).

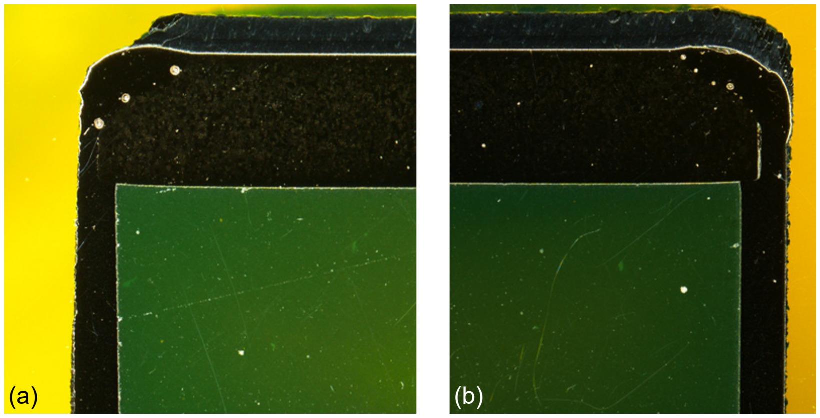

Figure 13.—Cross section photographs of the downstream end of the neutralizer keeper tube. (a) Beam side of the keeper, showing net erosion of the tube wall. (b) Opposite side of the keeper shown for comparison, displaying deposition.

Based on the measurements at the furthest downstream location, approximately 24 percent of the tube wall thickness had been eroded by the end of the test. However, these measurements were taken in the area of the weld between the orifice plate and the tube, which is downstream of the cathode orifice plate and heater. Upstream of the keeper orifice plate, the maximum eroded depth was approximately 17 percent of the pretest tube thickness, with erosion observed up to 2.5 plate thicknesses upstream of the downstream face of the keeper orifice plate. By comparison, the maximum erosion observed during the NEXT 2 kh wear test was 7.5 percent of the pretest tube thickness, with erosion observed up to 6.7 plate thicknesses upstream. Thus, there is a significant reduction in the extent of erosion observed in the NEXT LDT. The primary factor responsible for this difference is likely the reduced beam extraction diameter between the engineering model optics (used in the NEXT 2 kh wear test) and prototype model optics (used in the NEXT LDT). This effectively decreased the keeper tube area exposed to the ion beam, as well as reduced the overall ion flux to the surface. Furthermore, the flight design of the keeper incorporates a tube wall that is 50 percent thicker than what was tested in the NEXT LDT. This change, coupled with the reduced erosion rates observed during the NEXT LDT, indicates that keeper wear through should not be a life limiter for the thruster.

Other than the net erosion region observed near the downstream end of the keeper tube, deposition was found on the tube surface. A relatively uniform thin layer that was approximately 12 percent of the keeper tube thickness was found on the keeper tube wall, and was determined by EDS analysis to be primarily backsputtered carbon from the facility. However, the deposition on the beam side of the keeper exhibited a slightly different structure. Figure 15 shows a BSE image of the deposition, illustrating a thin layer of material in the middle with a distinctly different composition. While most of the deposition was found to be composed of backsputtered carbon from the facility, the thin layer was determined to have a high concentration of grid material. Given its location within the deposition thickness, this layer is likely the result of throttling the thruster to an operating condition with a higher degree of accelerator grid aperture erosion and a lower facility backsputter rate. While this deposition is not expected to cause any issues, it indicates that the keeper tube surface facing the beam will likely collect deposition from the grid in flight.

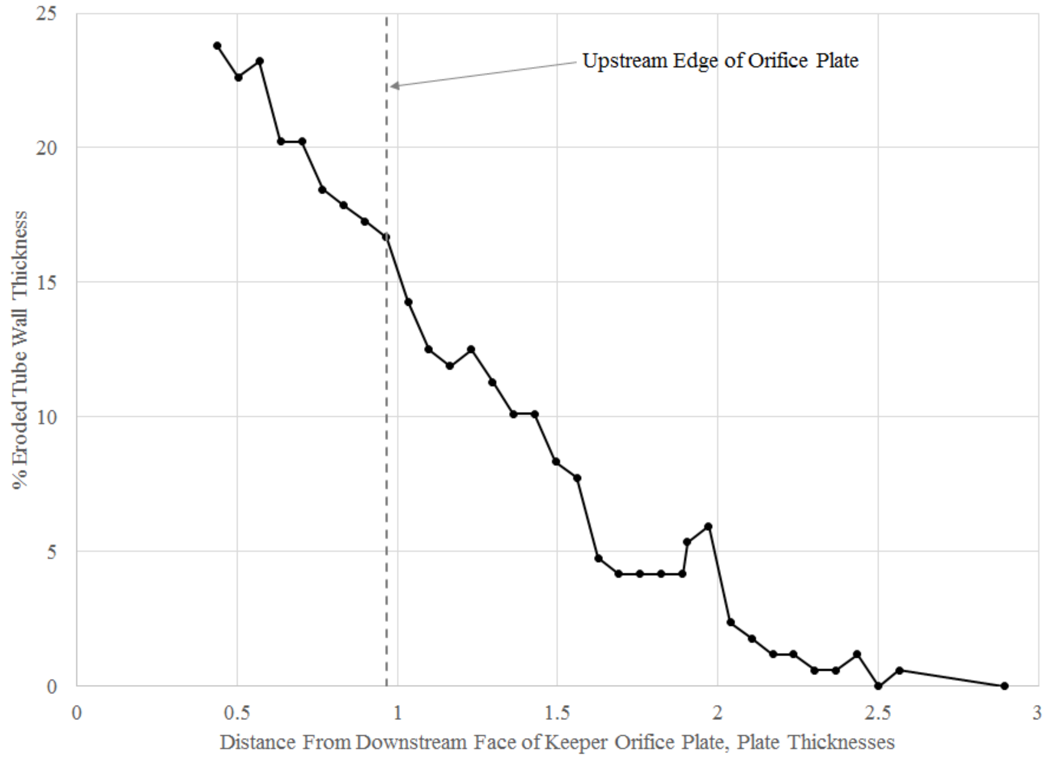

Figure 14.—Extent of erosion of the beam-side of the keeper tube wall as a function of upstream axial distance. The location of the upstream surface of the orifice plate is provided for reference.

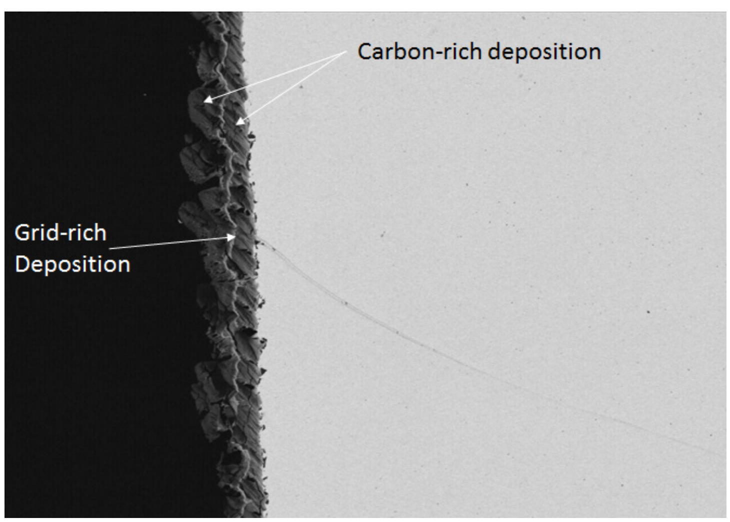

Figure 15.—Backscattered electron photomicrograph of the deposition layer on the beam side of the neutralizer keeper. A thin layer of grid-rich deposition was found within the primarily carbon-rich layer that had originated from the facility.

4.2.3 Neutralizer Cathode Orifice Plate and Tube

After the keeper was removed from the NCA, the cathode orifice plate and tube were visually inspected. Texturing of the orifice plate was observed, especially on the side closer to the ion beam. A closer inspection of this surface revealed the texturing to be pitting on much of the surface exposed by the keeper orifice plate (see Figure 16 and Figure 17). The photomicrograph shown in Figure 17 also shows signs of surface melting in the vicinity of the pits, which is another indication that perhaps arcing had occurred to the orifice plate. The weld between the orifice plate and cathode tube was found to be intact. Inspection of previously tested neutralizers with NEXT, including both engineering model and prototype model hardware, have also shown signs of pitting and/or arcing, although not as extensive as what is observed in the NEXT LDT. It is unclear at this time whether such pitting was observed on the neutralizer tested in the NSTAR ELT.

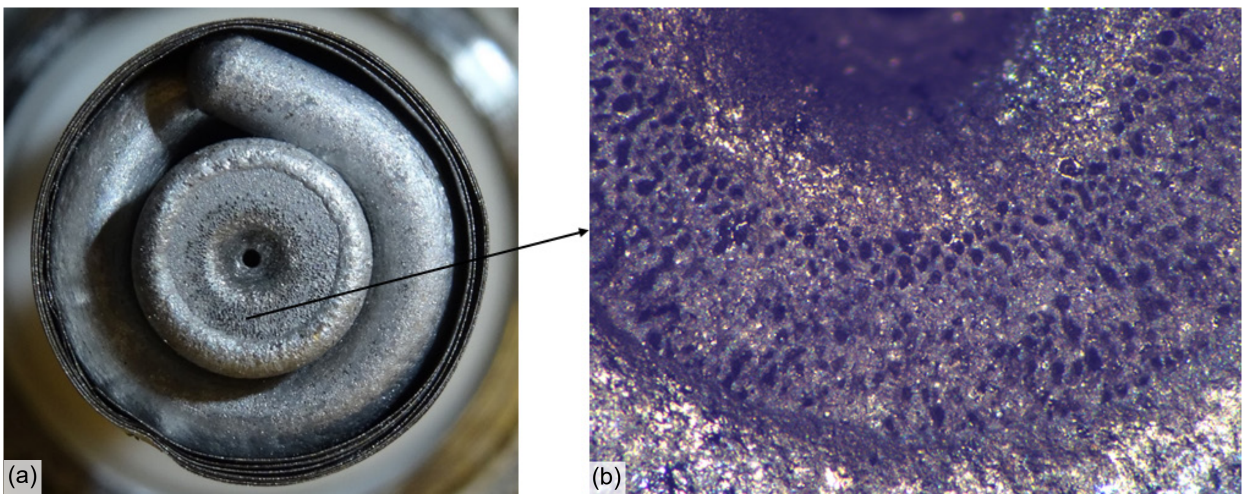

Figure 16.—Photographs of the neutralizer cathode orifice plate with keeper removed. (a) Overall front view of the orifice plate, showing signs of texturing. The side closer to the ion beam is at the bottom. (b) Close-up view of texturing, revealing numerous tiny pits in the surface.

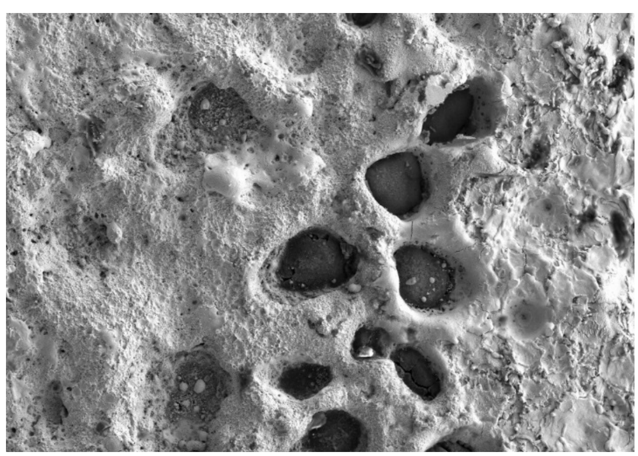

Figure 17.—Scanning electron microscopy photomicrograph of a pitted area on the neutralizer cathode orifice plate. Signs of surface melting are also present around the pits, potentially indicating that arcing had occurred.

It is speculated that this arcing had occurred during thruster recycles. During a recycle, it was found that the accelerator grid reaches potentials as high as the beam voltage. Large currents were also measured during a recycle as the beam power supply output capacitor discharged. These currents were found not only through the accelerator grid line, but also through the neutralizer common line leading back to the beam power supply. This indicates that a current path exists from the accelerator grid to the neutralizer as the beam power supply capacitor discharges during a recycle. Furthermore, visual observations of recycles occurring during the LDT around 30 kh revealed sparks occurring in the vicinity of the accelerator grid while the neutralizer plume became very bright and expanded. Depending on the size of this current and how it is carried, there may be ablation or arcing on the cathode orifice plate. While this was an unexpected observation, this arcing and resulting pitting did not prevent thruster operation or cause any issues regarding performance or lifetime. Furthermore, it is shown below that the pitting is highly superficial and did not significantly reduce the thickness of the orifice plate.

Non-contact profilometry was performed on the neutralizer cathode orifice plate across four different diameters. The minimum orifice diameter was also measured using a non-contact technique to be 8 percent smaller than the pretest diameter. This is consistent with in situ measurements of the orifice diameter taken prior to venting the thruster to atmosphere (Ref. 22). The orifice plate and cathode tube were then mounted in epoxy to preserve deposition and sectioned along the tube centerline. Figure 18 shows a scanning electron microscopy (SEM) photomicrograph of the cross-sectioned neutralizer cathode orifice. Also shown for reference is the nominal pretest orifice geometry. Significant erosion of the chamfer had occurred, with no well-defined downstream edge. Non-contact measurements of the downstream diameter indicate that in situ measurements of chamfer diameter were likely tracking the inner edge of the curved surface. Net deposition, determined by EDS analysis to be primarily material from either the cathode insert or the cathode orifice plate, was found on the upstream portion of the orifice barrel. However, no cathode impregnate materials (i.e., barium, calcium, or aluminum) were found in the deposition. Regions that exhibit net erosion also appear to be somewhat porous near the surface, indicating either redeposition of orifice plate/cathode insert material or surface pitting similar to what was observed on the downstream face. No significant change in the overall thickness of the orifice plate was found.

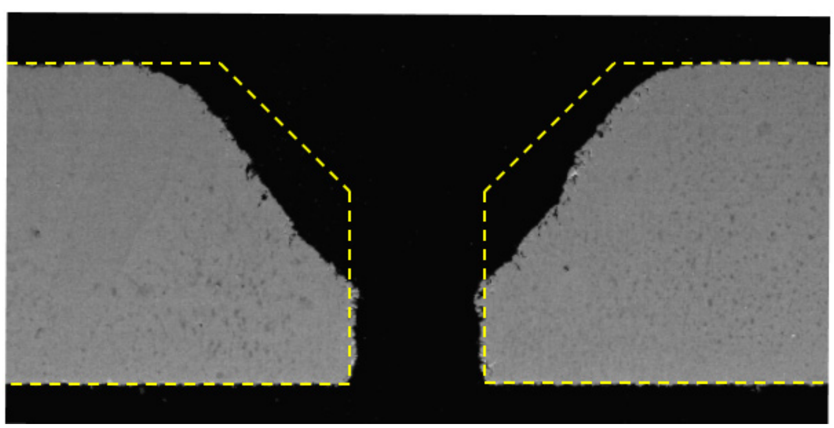

Figure 18.—Scanning electron microscopy photomicrograph of the NCA cathode orifice taken during post-test inspection. Dashed lines indicate the nominal pretest geometry.

No deposits were found within the neutralizer cathode orifice of the NEXT 2 kh wear test. However, given the relatively small amount of deposition found in the NEXT LDT, it is possible that the thruster was not operated long enough during the 2 kh wear test to observe such deposition. Furthermore, in situ measurements of the orifice diameter taken during the test indicate that the diameter did not decrease until the final segment at full power (after 29.2 kh) (Ref. 22). The overall orifice shape shown in Figure 18 differs from the final geometry of the neutralizer cathode orifice in the NSTAR ELT. At the end of the ELT, much of the original chamfer remained intact, with an enlargement or "fluting" of the majority of the cylindrical orifice upstream of the chamfer (Ref. 41). The reason for this difference is presently unknown, although the two cathodes do have slightly different dimensions and operate at different emission currents.

Prior to the post-test inspection, it had been speculated that changes to the neutralizer cathode orifice geometry due to wear were responsible for the observed loss in neutralizer performance during the NEXT LDT (Ref. 37). Cathode simulations performed at the Jet Propulsion Laboratory had shown that a general enlargement of the orifice would lead to a drop in keeper-to-cathode voltage, which accompanied the loss in flow margin (Refs. 37 and 47). Furthermore, the deposits found in the neutralizer keeper orifice as well as the in situ measurements of the cathode orifice chamfer diameter indicate that much of the erosion on the cathode orifice plate occurred during the first 19.5 kh when the greatest loss in neutralizer performance was observed. These findings support the theory that the cathode orifice erosion is responsible for the observed loss in neutralizer flow margin from plume mode. It is worth noting that while this loss was unexpected during the test, it has been resolved by cathode geometry changes implemented in the flight design as well as neutralizer mass flow changes to the latest NEXT throttle table (Ref. 37). These changes allow for adequate flow margin throughout the service life of the thruster.

The interior of the tube and upstream surface of the orifice plate were also inspected before and after sectioning had occurred. In certain regions along the inner tube wall, a thin layer of deposition approximately 5 to 10 µm thick was found, determined by EDS analysis to be composed of material from the cathode tube and insert. This was not unexpected given the proximity between the tube and the cathode insert in this region.

4.2.4 Neutralizer Cathode Radiation Shield and Heater

The neutralizer heater and radiation shield were also inspected after the keeper was removed from the assembly. The majority of the radiation shield was found to be excellent condition. However, signs of arcing were found near the downstream edge of the shield (see Figure 19). These arc tracks were limited to the outermost surface of the radiation shield. Furthermore, texturing of the downstream edge itself was observed (see Figure 16(a)). These features are likely correlated with the pitting observed on the downstream surface of the cathode orifice plate (see the previous section). Inspection of the radiation shield from the NEXT 2 kh wear test revealed similar arcing had occurred near the downstream edge, although to a much less degree likely due to the significantly lower run time. As with the pitting, it is unclear at this time whether these signs of arcing were observed on the NSTAR ELT hardware.

Inspection of the heater also revealed texturing on the downstream face (see Figure 16(a)). Aside from this, an inspection of the heater coil indicated it is in excellent condition (see Figure 20), with both heater terminations remaining intact. Post-test measurements of the heater resistance yielded an average value of 0.260 Ω, which is an 8.6 percent increase from the pretest average measurement of 0.240 Ω. This increase is surprising given that the neutralizer was only ignited 348 times during the test, and the heater voltage increased by at most a few percent during that time. It is possible that contact resistances in the circuit had artificially increased the overall measured resistance, even though the resistance of the measurement leads were accounted for. Indeed, the cathode heater resistance during initial inspection and disassembly

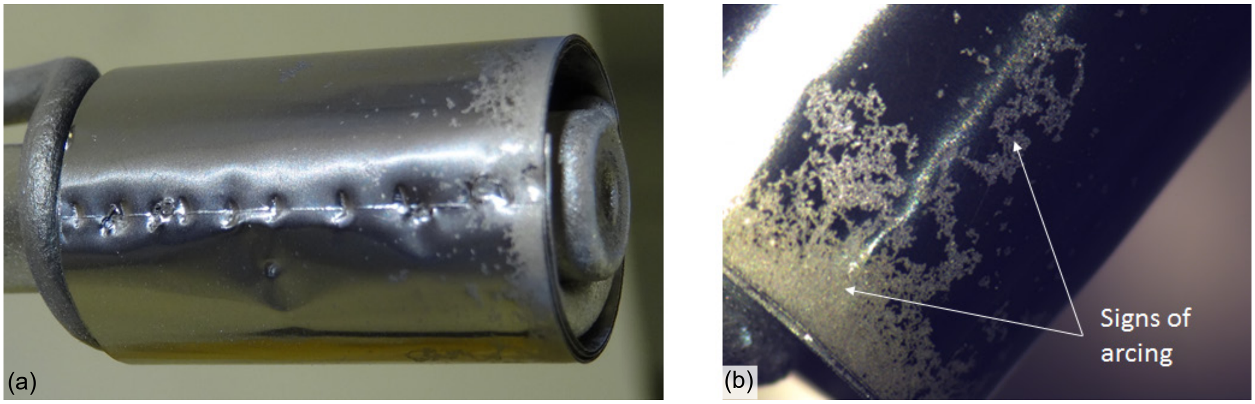

Figure 19.—Photographs of the heater radiation shield taken after the neutralizer keeper was removed. (a) Overall view of the radiation shield, showing that the majority of the outer surface is in excellent condition. (b) Close-up view of the downstream area that shows signs of arcing.

Figure 20.—Photograph of the heater coil after removal from the neutralizer cathode tube. Aside from texturing on the downstream face, the coil was found to be in excellent condition.

(at the ends of long thruster electrical lines) was found to increase with time. Regardless, no issues with the heater were observed during ignitions over the course of the test. The friction fit connecting the heater sheath to the cathode tube was secure, and removing the heater required some force. This is in contrast to the discharge cathode heater, which was easily removed from the tube and had exhibited intermittent heater open circuit behavior during the NEXT LDT.

4.2.5 Low Voltage Propellant Isolator

An impedance degradation between the neutralizer cathode common and facility ground was observed during the NEXT LDT, sometimes dropping to as low as 10 kΩ. While this did not have any measurable impact on thruster operation or performance, one of the objectives of the post-test inspection was to determine the source of the degradation. During the post-test inspection, the source of the low impedance was traced to the low voltage propellant isolator (LVPI), responsible for isolating the propellant flow line of the neutralizer from ground. The cross-sectioned LVPI revealed deposits on the insulator that led to the low impedance (see Figure 21). Analysis of these deposits with EDS indicated that they had come from the metallic ends of the LVPI. Signs of arcing were also found on the inside surfaces of the LVPI ends that face the insulator.

Low impedance between neutralizer and facility ground was also observed during the NSTAR ELT, but were caused by other factors besides the LVPI (Ref. 41). Inspection of the LVPI hardware from the NEXT 2 kh wear test also revealed deposits on the insulator similar to the LDT. It is speculated that the

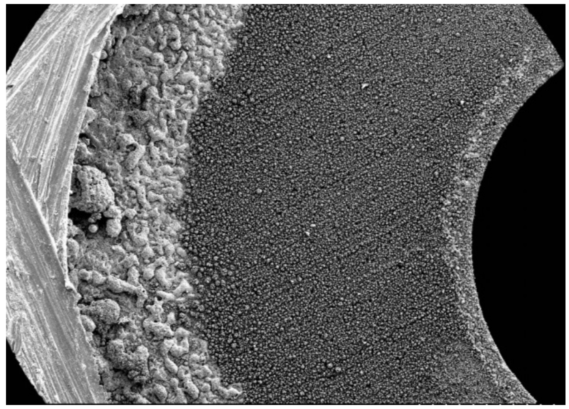

Figure 21.—Scanning electron microscopy photomicrograph of the upstream side of the insulator within the NEXT LDT LVPI. Significant deposits were found, resulting in a low impedance path.

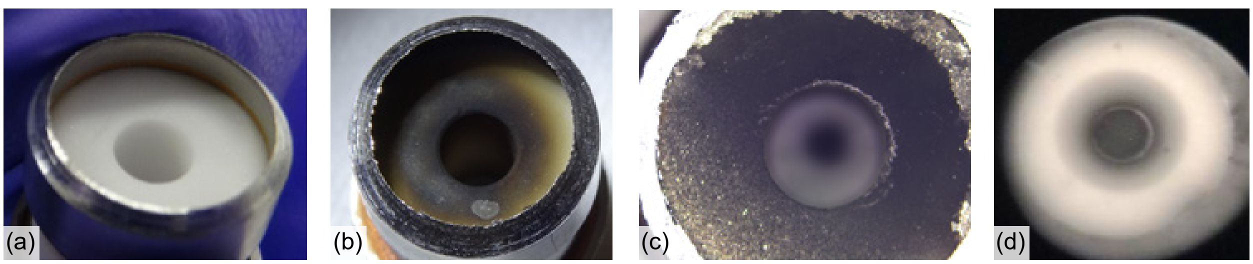

Figure 22.—Photographs of the upstream surface of the insulator within various NEXT LVPIs. (a) Unused engineering model LVPI. (b) LVPI from the NEXT 2 kh wear test. (c) LVPI from the NEXT LDT. (d) LVPI on the NEXT prototype model thruster (taken in situ with a borescope).

arcing occurs during thruster recycles, where the dense plasma within the neutralizer cathode can be created upstream to the LVPI and seed a discharge across the insulator. A shield is placed within the LVPI to prevent plasma from migrating upstream to the insulator. However, both tests used engineering model isolators, which contained shields that had a relatively high open-area fraction. The LVPI on the prototype model NEXT thruster has a shield with a much lower open-area fraction. A borescope inspection of the LVPI insulator on the prototype model NEXT thruster shows no sign of arcing despite having over 2,000 h of operation (see Figure 22). These results indicate that the flight design of the LVPI should prevent arcing across the insulator, and thus impedance degradation between the neutralizer and ground should not occur.

5.0 Summary and Future Work

The NEXT LDT is part of a comprehensive thruster service life assessment intended to demonstrate overall throughput capability, validate service life models, quantify wear rates as a function of time and operating condition, and identify any unknown life-limiting mechanisms. In February 2014, the test was voluntarily terminated after demonstrating 51,184 h of high-voltage operation, 918 kg of propellant throughput, and 35.5 MN-s of total impulse. Post-test inspection began shortly afterwards and was focused on measuring critical thruster wear rates that can induce thruster failure to verify both in situ measurements and the service life model predictions, resolving any thruster-related issues encountered during the NEXT LDT, verifying that thruster design changes made as a result of prior wear test findings had the desired impacts, and identifying any unanticipated life-limiting phenomena. As of this publication, the post-test inspection is nearing completion and the results with design improvements will be delivered to GRC's industry partner Aerojet Rocketdyne as they develop and build two NEXT flight thrusters and PPUs.

Both discharge and neutralizer cathodes were thoroughly inspected using non-destructive and destructive techniques. For the discharge cathode, a maximum keeper erosion depth of only 16 percent of the orifice plate thickness was found, indicating ample remaining lifetime and a marked improvement over wear rates observed during the NEXT 2 kh wear test and the NSTAR ELT. The downstream surface of the cathode orifice plate exposed to the plasma exhibited significant erosion, but all other cathode components including the rest of the orifice plate, heater, and radiation shield were found to be in remarkably good condition. This is a consequence of the observed low erosion rates of the keeper, which had adequately protected vital cathode components throughout the 51 kh life test. Eroded products from the cathode orifice plate were found in the inter-electrode gap that were responsible for the observed keeper-to-cathode electrical short during the test. Data indicate that the only significant impact of this short is a ~ 2 min increase in typical cathode ignition times, although this impact may be reduced with a flight-like ignitor pulse and environment. The observed discharge heater open circuit during the test is attributed to poor contact between the heater sheath and cathode tube during ignitions, which is being addressed in the cathode flight design.

For the neutralizer cathode, erosion of the beam side of the keeper tube was significantly reduced compared to the results from the NEXT 2 kh wear test. This has been attributed to the reduced beam extraction diameter, which decreases the ion beam flux to the neutralizer keeper surface. Significant deposition was observed within the keeper orifice as well as the downstream face, which may have affected the measured flow margin from plume mode during the test. Because this deposition was primarily facility-induced, its impact on the measurements will need to be assessed. Significant erosion of the neutralizer cathode orifice was found, with the shape of the orifice differing from what was observed in the NSTAR ELT. Despite this difference, strong evidence remains that the enlargement of the orifice is responsible for the loss in neutralizer performance observed during the test. This loss has been mitigated by geometric changes to the neutralizer flight design, as well as neutralizer flow rate changes in the latest NEXT throttle table. Evidence of arcing at the neutralizer was found on the cathode orifice plate as well as near the downstream edge of the heater radiation shield. This arcing is believed to occur during thruster recycles, when the accelerator grid can reach the beam voltage and current was measured to flow between the neutralizer and the accelerator grid. The resulting pitting and arc tracks were superficial and not expected to be an issue. Lastly, an observed low impedance between neutralizer and facility ground was determined to be caused by arcing within the low voltage propellant isolator. A design change between the isolator used in the LDT and the flight-like model used in the prototype thruster appears to have solved this issue and is therefore not a concern.

A few tasks remain to be completed for the post-test inspection of the cathodes. In particular, the cathode inserts must be inspected for barium depletion as well as any tungstate formation. Also, further inspection of both heaters is being considered. This will either entail sectioning the heaters and inspecting the cross sections of each coil, or operating them in a cyclic heater life test to quantify their remaining lifetime. Finally, all these data will be used to validate and update the thruster service life models, which will complete the service life assessment for the NEXT thruster.

References

1. Brophy, J. R., et al., "Development and Testing of the Dawn Ion Propulsion System," *42nd AIAA/ASME/SAE/ASEE Joint Propulsion Conference and Exhibit*, AIAA-2006-4319, Sacramento, CA, July 9-12, 2006.
2. Patterson, M. J. and Benson, S. W., "NEXT Ion Propulsion System Development Status and Performance," *43rd AIAA/ASME/SAE/ASEE Joint Propulsion Conference and Exhibit*, AIAA-2007-5199, Cincinnati, OH, July 8-11, 2007.
3. Polk, J. E., et al., "Demonstration of the NSTAR Ion Propulsion System on the Deep Space One Mission," *27th International Electric Propulsion Conference*, IEPC-2001-075, Pasadena, CA, October 15-19, 2001.
4. Rayman, M. D., "The Successful Conclusion of the Deep Space 1 Mission: Important Results Without a Flashy Title," *Space Technology*, Vol. 23, No. 2-3, 2003, pp. 185-196.
5. Benson, S. W. and Patterson, M. J., "NASA's Evolutionary Xenon Thruster (NEXT) Ion Propulsion Technology Development Status in 2009," *31st International Electric Propulsion Conference*, IEPC-2009-150, Ann Arbor, MI, September 20-24, 2009.
6. Hoskins, W. A., Aadland, R. S., Meckel, N. J., Talerico, L. A., and Monheiser, J. M., "NEXT Ion Propulsion System Production Readiness," *43rd AIAA/ASME/SAE/ASEE Joint Propulsion Conference and Exhibit*, AIAA-2007-5856, Cincinnati, OH, July 8-11, 2007.
7. Patterson, M. J., et al., "NEXT Multi-Thruster Array Test - Engineering Demonstration," *42nd AIAA/ASME/SAE/ASEE Joint Propulsion Conference and Exhibit*, AIAA-2006-5180, Sacramento, CA, July 9-12, 2006.
8. Snyder, J. S., Anderson, J. R., Van Noord, J. L., and Soulas, G. C., "Environmental Testing of the NEXT PM1 Ion Engine," *43rd AIAA/ASME/SAE/ASEE Joint Propulsion Conference and Exhibit*, AIAA-2007-5275, Cincinnati, OH, July 8-11, 2007.
9. Soulas, G. C., Patterson, M. J., Pinero, L., Herman, D. A., and Snyder, J. S., "NEXT Single String Integration Test Results," *45th AIAA/ASME/SAE/ASEE Joint Propulsion Conference and Exhibit*, AIAA-2009-4816, Denver, CO, August 2-5, 2009.
10. Aadland, R. S., Frederick, H., Benson, S. W., and Malone, S. P., "Development Results of the NEXT Propellant Management System," *JANNAF 2nd Liquid Propulsion Subcommittee and 1st Spacecraft Propulsion Subcommittee Joint Meeting*, JANNAF 2005-0356DW, Monterey, CA, December 5-8, 2005.
11. Crofton, M. W., et al., "Characterization of the NASA NEXT Thruster," *45th AIAA/ASME/SAE/ASEE Joint Propulsion Conference and Exhibit*, AIAA-2009-4815, Denver, CO, August 2-5, 2009.
12. Diamant, K. D., Pollard, J. E., Crofton, M. W., Patterson, M. J., and Soulas, G. C., "Thrust Stand Characterization of the NASA NEXT Thruster," *46th AIAA/ASME/SAE/ASEE Joint Propulsion Conference & Exhibit*, AIAA-2010-6701, Nashville, TN, July 25 - 28, 2010.
13. Herman, D. A., Pinero, L. R., and Sovey, J. S., "NASA's Evolutionary Xenon Thruster (NEXT) Component Verification Testing," *44th AIAA/ASME/SAE/ASEE Joint Propulsion Conference and Exhibit*, AIAA-2008-4812, Hartford, CT, July 21-23, 2008.
14. Herman, D. A., Soulas, G. C., and Patterson, M. J., "Performance Evaluation of the Prototype-Model NEXT Ion Thruster," *43rd AIAA/ASME/SAE/ASEE Joint Propulsion Conference and Exhibit*, AIAA-2007-5212, Cincinnati, OH, July 8-11, 2007.
15. Pinero, L. R., Hopson, M., Todd, P. C., and Wong, B., "Performance of the NEXT Engineering Model Power Processing Unit," *43rd AIAA/ASME/SAE/ASEE Joint Propulsion Conference and Exhibit*, AIAA-2007-5214, Cincinnati, OH, July 8-11, 2007.

16. Pollard, J. E., Diamant, K. D., Crofton, M. W., Patterson, M. J., and Soulas, G. C., “Spatially-Resolved Beam Current and Charge-State Distributions for the NEXT Ion Engine,” *46th AIAA/ASME/SAE/ASEE Joint Propulsion Conference and Exhibit*, AIAA-2010-6779, Nashville, TN, July 25-28, 2010.
17. Snyder, J. S., et al., “Vibration Test of a Breadboard Gimbal for the NEXT Ion Engine,” *42nd AIAA/ASME/SAE/ASEE Joint Propulsion Conference and Exhibit*, AIAA-2006-4665, Sacramento, CA, July 9-12, 2006.
18. Van Noord, J. L., “Lifetime Assessment of the NEXT Ion Thruster,” *43rd AIAA/ASME/SAE/ASEE Joint Propulsion Conference and Exhibit*, AIAA-2007-5274, Cincinnati, OH, July 8-11, 2007.
19. Van Noord, J. L. and Herman, D. A., “Application of the NEXT Ion Thruster Lifetime Assessment to Thruster Throttling,” *44th AIAA/ASME/SAE/ASEE Joint Propulsion Conference and Exhibit*, AIAA-2008-4526, Hartford, CT, July 21-23, 2008.
20. Soulas, G. C., Kamhawi, H., Patterson, M. J., Britton, M. A., and Frandina, M. M., “NEXT Ion Engine 2000 Hour Wear Test Results,” *40th AIAA/ASME/SAE/ASEE Joint Propulsion Conference and Exhibit*, AIAA-2004-3791, Fort Lauderdale, FL, July 11-14, 2004.
21. Van Noord, J. L., Soulas, G. C., and Sovey, J. S., “NEXT PM1R Ion Thruster and Propellant Management System Wear Test Results,” *31st International Electric Propulsion Conference*, IEPC-2009-163, Ann Arbor, MI, September 20-24, 2009.
22. Shastry, R., Herman, D. A., Soulas, G. C., and Patterson, M. J., “End-of-test Performance and Wear Characterization of NASA's Evolutionary Xenon Thruster (NEXT) Long-Duration Test,” *50th AIAA/ASME/SAE/ASEE Joint Propulsion Conference*, AIAA-2014-3617, Cleveland, OH, July 28-30, 2014.
23. Soulas, G. C. and Shastry, R., “Post-test Inspection of NASA's Evolutionary Xenon Thruster Long Duration Test Hardware: Ion Optics,” *52nd AIAA/SAE/ASEE Joint Propulsion Conference*, Salt Lake City, UT, July 25 - 27, 2016 (to be published).
24. Shastry, R. and Soulas, G. C., “Post-test Inspection of NASA's Evolutionary Xenon Thruster Long-Duration Test Hardware: Discharge Chamber,” *52nd AIAA/SAE/ASEE Joint Propulsion Conference*, Salt Lake City, UT, July 25 - 27, 2016 (to be published).
25. Hoskins, W. A., et al., “Development of a Prototype Model Ion Thruster for the NEXT System,” *40th AIAA/ASME/SAE/ASEE Joint Propulsion Conference and Exhibit*, AIAA-2004-4111, Fort Lauderdale, FL, July 11-14, 2004.
26. Soulas, G. C. and Patterson, M. J., “NEXT Ion Thruster Performance Dispersion Analyses,” *43rd AIAA/ASME/SAE/ASEE Joint Propulsion Conference and Exhibit*, AIAA-2007-5213, Cincinnati, OH, July 8-11, 2007.
27. Frandina, M. M., Arrington, L. A., Soulas, G. C., Hickman, T. A., and Patterson, M. J., “Status of the NEXT Ion Thruster Long Duration Test,” *41st AIAA/ASME/SAE/ASEE Joint Propulsion Conference and Exhibit*, AIAA-2005-4065, Tucson, AZ, July 10-13, 2005.
28. Herman, D. A., Soulas, G. C., and Patterson, M. J., “Performance Characteristics of the NEXT Long-Duration Test after 16,550 h and 337 kg of Xenon Processed,” *44th AIAA/ASME/SAE/ASEE Joint Propulsion Conference and Exhibit*, AIAA-2008-4527, Hartford, CT, July 21-23, 2008.
29. Herman, D. A., Soulas, G. C., and Patterson, M. J., “NEXT Long-Duration Test Plume and Wear Characteristics after 16,550 h of Operation and 337 kg of Xenon Processed,” *44th AIAA/ASME/SAE/ASEE Joint Propulsion Conference and Exhibit*, AIAA-2008-4919, Hartford, CT, July 21-23, 2008.
30. Patterson, M. J., et al., “NEXT: NASA's Evolutionary Xenon Thruster,” *38th AIAA/ASME/SAE/ASEE Joint Propulsion Conference and Exhibit*, AIAA-2002-3832, Indianapolis, IN, July 7-10, 2002.

31. Soulas, G. C., Domonkos, M. T., and Patterson, M. J., "Performance Evaluation of the NEXT Ion Engine," *39th AIAA/ASME/SAE/ASEE Joint Propulsion Conference and Exhibit*, AIAA-2003-5278, Huntsville, AL, July 20-23, 2003.
32. Herman, D. A., Soulas, G. C., and Patterson, M. J., "Status of the NEXT Long-Duration Test after 23,300 Hours of Operation," *45th AIAA/ASME/SAE/ASEE Joint Propulsion Conference and Exhibit*, AIAA-2009-4917, Denver, CO, August 2-5, 2009.
33. Herman, D. A., "Status of the NASA's Evolutionary Xenon Thruster (NEXT) Long-Duration Test after 30,352 Hours of Operation," *46th AIAA/ASME/SAE/ASEE Joint Propulsion Conference and Exhibit*, AIAA-2010-7112, Nashville, TN, July 25 - 28, 2010.
34. Herman, D. A., "NASA's Evolutionary Xenon Thruster (NEXT) Project Qualification Propellant Throughput Milestone: Performance, Erosion, and Thruster Service Life Prediction after 450 kg," *JANNAF 7th Modeling and Simulation, 5th Liquid Propulsion, and 4th Spacecraft Propulsion Joint Subcommittee Meeting*, CPIAC JSC 2010-0015EH and NASA TM-2010-216816, Colorado Springs, CO, May 3-7, 2010.
35. Herman, D. A., "Review of the NASA's Evolutionary Xenon Thruster (NEXT) Long-Duration Test as of 632 kg of Propellant Throughput," *47th AIAA/ASME/SAE/ASEE Joint Propulsion Conference and Exhibit*, AIAA-2011-5658, San Diego, CA, July 31 - August 3, 2011.
36. Herman, D. A., Soulas, G. C., and Patterson, M. J., "Status of the NEXT Ion Thruster Long-Duration Test after 10,100 h and 207 kg Demonstrated," *43rd AIAA/ASME/SAE/ASEE Joint Propulsion Conference and Exhibit*, AIAA-2007-5272, Cincinnati, OH, July 8-11, 2007.
37. Herman, D. A., Soulas, G. C., and Patterson, M. J., "NEXT Long-Duration Test Neutralizer Performance and Erosion Characteristics," *31st International Electric Propulsion Conference*, IEPC-2009-154, Ann Arbor, MI, September 20-24, 2009.
38. Herman, D. A., Soulas, G. C., Van Noord, J. L., and Patterson, M. J., "NASA's Evolutionary Xenon Thruster Long-Duration Test Results," *Journal of Propulsion and Power*, Vol. 28, No. 3, May - June, 2012, pp. 625-635.
39. Shastry, R., Herman, D. A., Soulas, G. C., and Patterson, M. J., "NASA's Evolutionary Xenon Thruster (NEXT) Long-Duration Test as of 736 kg of Propellant Throughput," *48th AIAA/ASME/SAE/ASEE Joint Propulsion Conference and Exhibit*, AIAA-2012-4023, Atlanta, GA, July 29 - August 1, 2012.
40. Shastry, R., Herman, D. A., Soulas, G. C., and Patterson, M. J., "Status of NASA's Evolutionary Xenon Thruster (NEXT) Long-Duration Test as of 50,000 h and 900 kg Throughput," *33rd International Electric Propulsion Conference*, IEPC-2013-121, Washington D.C., October 6 - 10, 2013.
41. Sengupta, A., et al., "The 30,000-Hour Extended-Life Test of the Deep Space 1 Flight Spare Ion Thruster," NASA/TP 2004-213391, March, 2005.
42. Polk, J. E., et al., "An Overview of the Results from an 8200 Hour Wear Test of the NSTAR Ion Thruster," *35th AIAA/ASME/SAE/ASEE Joint Propulsion Conference and Exhibit*, AIAA-1999-2446, Los Angeles, CA, June 20-24, 1999.
43. Britton, M., Soulas, G. C., Kamhawi, H., and Snyder, A., "Destructive Analysis of the NEXT 2000-Hour Wear Test Hollow Cathode Assemblies," NASA/TM-2005-213387, July, 2005.
44. Williams, G. J., et al., "Results of the 2000 hr Wear Test of the HiPEP Ion Thruster with Pyrolytic Graphite Ion Optics," *42nd AIAA/ASME/SAE/ASEE Joint Propulsion Conference and Exhibit*, AIAA-2006-4668, Sacramento, CA, July 9-12, 2006.
45. Thomas, R. E., *Personal Communication*. 2016: Glenn Research Center.

46. Garner, C. E. and Rayman, M. D., "In-Flight Operation of the Dawn Ion Propulsion System Through Survey Science Orbit at Ceres," *51st AIAA/SAE/ASEE Joint Propulsion Conference*, AIAA-2015-3717, Orlando, FL, July 27 - 29, 2015.
47. Mikellides, I. G., Snyder, J. S., Goebel, D. M., Katz, I., and Herman, D. A., "Neutralizer Hollow Cathode Simulations and Comparisons with Ground Test Data," *31st International Electric Propulsion Conference*, IEPC-2009-20, Ann Arbor, MI, September 20-24, 2009.